Cooling of the Arctic and Antarctic Polar Stratospheres due to Ozone Depletion

WILLIAM J. RANDEL AND FEI WU

National Center for Atmospheric Research, Boulder, Colorado

(Manuscript received 13 January 1998, in final form 17 July 1998)

ABSTRACT

Long time records of stratospheric temperatures indicate that substantial cooling has occurred during spring over polar regions of both hemispheres. These cooling patterns are coincident with observed recent ozone depletions. Time series of temperature from radiosonde, satellite, and National Centers for Environmental Prediction reanalysis data are analyzed in order to isolate the space–time structure of the observed temperature changes. The Antarctic data show strong cooling (of order 6–10 K) in the lower stratosphere (~12–21 km) since approximately 1985. The cooling maximizes in spring (October–December), with small but significant changes extending throughout Southern Hemisphere summer. No Antarctic temperature changes are observed during midwinter. Significant warming is found during spring at the uppermost radiosonde data level (30 mb, ~24 km). These observed temperature changes are all consistent with model predictions of the radiative response to Antarctic polar ozone depletion. Winter and spring temperatures in Northern Hemisphere polar regions also indicate a strong cooling in the 1990s, and the temperature changes are coherent with observed ozone losses. The overall space–time patterns are similar between both hemispheres, suggesting that the radiative response to ozone depletion is an important component of the Arctic cooling as well.

1. Introduction

Ground-based and satellite observations show a dramatic decrease in ozone over Antarctica during Southern Hemisphere (SH) spring since about 1980 (Farman et al. 1985; Stolarski et al. 1986). Characteristics of the so-called ozone hole are reviewed in Solomon (1988) and WMO (1995), and recent updates are provided in Jones and Shanklin (1995), Hofmann et al. (1997), and WMO (1999). It was realized shortly after the ozone hole was discovered that the loss of ozone would have an impact on the radiative equilibrium of the Antarctic stratosphere, such that a cooling of order ~5 K would be anticipated (Shine 1986). Simulations using sophisticated general circulation models confirmed this hypothesis, and suggested that the strongest cooling would occur in the lower stratosphere during late SH spring (Kiehl et al. 1988; Cariolle et al. 1990; Mahlman et al. 1994; Ramaswamy et al. 1996; Shindell et al. 1997; Graf et al. 1998).

Observations of long-term temperature variability in the Antarctic stratosphere have shown evidence of strong coupling between ozone and temperature. Angell (1986), Chubachi (1986), Newman and Schoeberl (1986), Sekiguchi (1986), Newman and Randel (1988), and Randel and Cobb (1994) all noted strong correlation between contemporaneous ozone and temperature variations during SH spring. This observed coherence spans high-frequency month-to-month variability [where the ozone–temperature correlations are due to dynamics; see Newman and Randel (1988) and Wirth (1993)], in addition to low-frequency decadal trends (where the temperature should respond radiatively to ozone changes). A decadal-scale cooling of the Antarctic stratosphere during spring has been noted in a number of observational studies (Trenberth and Olson 1989; Koshelkov et al. 1992; Hurrell and van Loon 1994; Jones and Shanklin 1995). Randel (1988) showed large temperature and circulation differences in the SH during spring 1987, in conjunction with the largest Antarctic ozone depletion observed up to that time. However, because ''natural'' year-to-year meteorological variability is a maximum in the Antarctic during SH spring (the same period as the ozone hole), it requires a relatively long record to isolate low-frequency decadal changes. [It turns out that the temperature anomalies shown in Randel (1988) are somewhat larger than the decadal variations shown here, because 1987 was a relatively quiescent dynamical year.] Since the ozone hole has been evident now for somewhat over a decade, it is possible to directly compare pre- versus post-ozone-hole time periods to study details of the decadal-scale temperature changes.

Although the Arctic polar stratospheric vortex displays a large degree of ''natural'' interannual variability during winter, the decade of the 1990s has exhibited

Corresponding author address: Dr. William J. Randel, Atmospheric Chemistry Division, National Center for Atmospheric Research, P.O. Box 3000, Boulder, CO 80307-3000.
E-mail: randel@ucar.edu

several particularly cold winters (namely 1993/94, 1994/95, and 1996/97; see Zurek et al. 1996; Pawson and Naujokat 1997; Coy et al. 1997). These cold years in the Northern Hemisphere (NH) have furthermore exhibited low ozone levels during winter and spring (Newman et al. 1997; Fioletov et al. 1997). The observed correlation between cold temperatures and low ozone in the Arctic is likely due to one or more of the following causes: 1) dynamically quiescent periods are associated with cold temperatures and reduction in ozone transport to polar regions, 2) cold temperatures lead to enhanced chemical ozone depletion, and 3) the radiative response to ozone loss results in colder temperatures. While in the case of Antartica it appears that temperatures are primarily responding to ozone loss (due to the agreement with ozone hole GCM simulations), the separation is not clear-cut in the Arctic (and indeed all of the above mechanisms are likely important).

The purpose of this work is to use long records of temperature observations to analyze the detailed space–time structure of the decadal-scale cooling observed in the Arctic and Antarctic. In particular, we aim to quantify the altitude structure of the cooling, and the detailed seasonality. For the Antarctic we utilize long records of radiosonde data for many stations that extend back to the late 1950s. We also use temperature records from the National Centers for Environmental Prediction (NCEP) global meteorological reanalyses (Kalnay et al. 1996), and satellite radiance measurements to examine both Antarctic and Arctic regions. The results show strong cooling of the Antarctic lower stratosphere in spring, and over the Arctic during winter–spring. The observed cooling in both hemispheres is statistically significant with respect to ''natural'' interannual variability. We furthermore compare the temperature changes to decadal-scale ozone depletion in both the NH and SH, and find strong space–time coherence. The good agreement with model calculations for the Antarctic suggests the temperatures are primarily responding to ozone loss. The overall similarity of observations between the NH–SH suggests that such a radiative response also contributes a large fraction of the observed Arctic cooling.

2. Data and analyses

a. Radiosondes

We analyze radiosonde observations from eight Antarctic stations with relatively long and continuous time records of lower-stratospheric data. These stations are shown below in Fig. 3, with time series extending back to approximately 1955–65 (depending on individual station). These radiosonde data provide reasonably complete records for the troposphere and lower stratosphere, for levels up to 50 or 30 mb, although some stations have regular missing observations during winter, or for certain subperiods [see Trenberth and Olsen (1989) for sampling details at Admundsen–Scott and McMurdo]. For altitudes above the 100-mb pressure level there is frequent loss of data during midwinter, due to balloon bursts. This is a common problem, and limits our analyses in the upper levels in midwinter.

We construct monthly temperature anomalies from the daily radiosonde data according to the method of Trenberth and Olson (1989). The daily data at each pressure level are fit to an annual cycle using a time mean plus four annual harmonics. The daily departures from this annual cycle are then averaged within each calendar month to produce monthly anomalies. The annual cycle is added back on if full temperature values are needed (with missing months still left blank).

b. NCEP reanalyses

We also analyze monthly mean temperatures from the NCEP reanalyses (Kalnay et al. 1996) with time series available spanning 1968–97. Time series of Antarctic radiosondes shown below also include NCEP reanalysis results interpolated to the station location for comparison. Statistical comparisons of these data over 1968–97 show mean differences (biases) between these data including 1) an NCEP warm bias of $\sim$2 K in the lower stratosphere during winter (as found also by Manney et al. 1996), and 2) NCEP cold biases (up to 3–8 K) for the east Antarctic coast stations (Syowa, Mawson, Davis, and Casey) in spring. Although there is reasonable agreement for interannual temperature variations between the NCEP reanalysis and Antarctic radiosondes at some stations, there are often large differences apparent for these same stations on the east Antarctic coast (see Fig. 3 below). Cross comparisons between stations give no reason to suspect the radiosonde data quality at these stations; rather, it is likely that there is some problem in the reanalysis for these locations. We also note an apparent discontinuity in reanalysis temperatures in the tropical lower stratosphere, probably due to the introduction of satellite data in 1978 (Mo et al. 1995).

c. MSU data

A homogeneous record of global lower-stratospheric temperature is available from the microwave sounding unit (MSU) channel 4 (Spencer and Christy 1993). Channel 4 measures the thermal radiation emitted from an atmospheric layer centered between approximately 50–150 mb (13–22 km), with a maximum response near 90 mb (17 km). We compare these satellite data with the radiosonde and reanalysis records, and find good overall agreement.

d. Decadal filtering

Figure 1 shows time series of October and December average 100-mb temperatures at Halley Bay from the radiosonde records and the NCEP reanalyses. Superimposed over the yearly time series in each plot is a

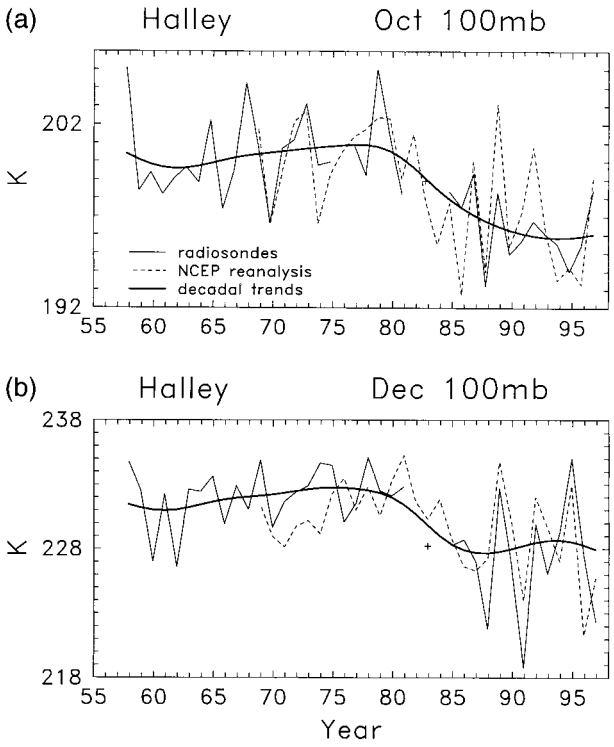

FIG. 1. Time series of 100-mb temperature at Halley Bay, Antartica, during (a) Oct and (b) Dec. Light solid lines are radiosonde data and dashed lines are from the NCEP reanalysis. The smoothed curve in each panel is the smoothed decadal variation [Eq. (1)] calculated from the radiosonde data.

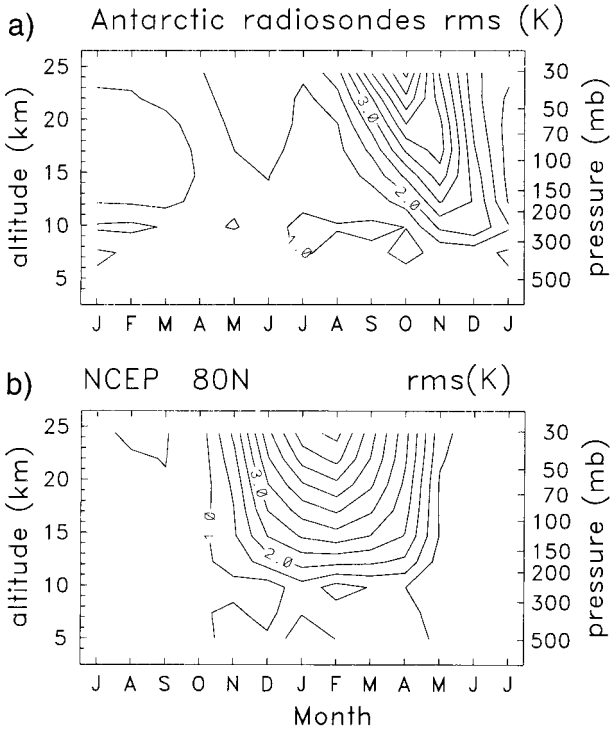

FIG. 2. Altitude–month profiles of rms interannual temperature anomalies [Eq. (2)] over (a) Antartica (top-derived from radiosonde data) and (b) over the Arctic (bottom-derived from NCEP reanalysis data at 80°N). These are estimates of the natural interannual variability of monthly means about the smoothed decadal trends. Note the time axes are shifted by 6 months to facilitate direct seasonal comparisons.

smoothed curve intended to highlight low-frequency, decadal-scale variations. These smooth time series in Fig. 1 clearly show a cooling at Halley Bay since about 1985 compared to pre-1980 climatology. The decadal-scale time series (T_d) are calculated from the monthly means by a running weighted average over adjacent years according to

$$T_d(i) = \sum_{j=-10}^{10} T(i + j)W(j). \qquad (1)$$

Here i and j are year indices, and $W(j)$ is a Gaussian-shaped smoothing filter, with a half-width of 4 yr [$W(j) = \exp(-(j/4)^2)$]. Besides highlighting decadal timescale variations, the weighting in Eq. (1) also provides a means of interpolating across short spans of missing radiosonde observations. Data on either end of the time series simply use one-sided weighting.

Estimates of natural, high-frequency interannual variability are used to calculate statistical significance for the decadal-scale changes. These are calculated by evaluating the year-to-year fluctuations about the smooth, decadal curves. The yearly rms deviation is calculated as

$$T_{\rm rms} = \left\{\frac{1}{N}\sum_{i=1}^{N}[T(i) - T_d(i)]^2\right\}^{1/2}. \qquad (2)$$

Figure 2a shows a contour plot of $T_{\rm rms}$ versus altitude and month of year for the Antarctic radiosonde data (averaged over the eight stations). This natural interannual variability shows a clear maximum (of order 3–5 K) during SH spring (September–December) in the stratosphere (altitudes above ~8 km). Figure 2b shows a similar calculation of $T_{\rm rms}$ for Arctic data (zonal means at 80°N), derived from the NCEP reanalysis. The natural interannual variability in the NH peaks during winter–spring (January–March), substantially earlier than that in the SH. However, the magnitude of the natural variability is similar between Arctic winter and Antarctic spring (~3–5 K).

Significant changes in the smoothed decadal-scale time series (T_d), or in simple 5- or 10-yr means, are evaluated using the year-to-year variability ($T_{\rm rms}$), together with the number of independent pieces of information (n) associated with the averaging. Specifically, the standard deviation (σ) of T_d is

$$\sigma = \left(\frac{T_{\rm rms}^2}{n - 1}\right)^{1/2}. \qquad (3)$$

The value of n for the Gaussian smoothing filter with half-width of 4 yr is 10 [evaluated using Blackman and

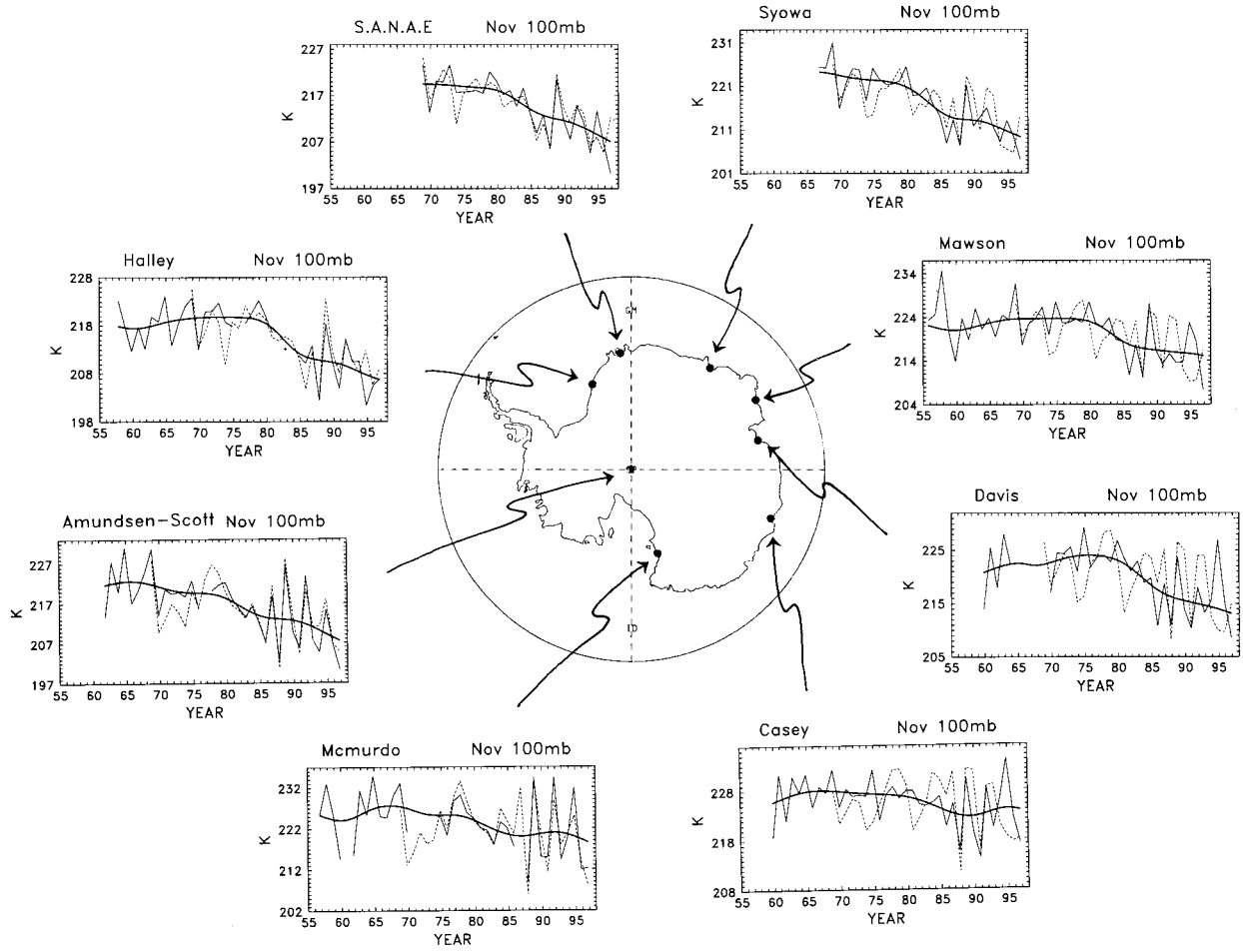

FIG. 3. Time series of Nov 100-mb temperatures at eight Antarctic radiosonde stations. Line patterns are the same as those in Fig. 1.

Tukey (1958, 24)]. Hence the σ appropriate to the decadal T_d changes is $T_{\rm rms}$ divided by 3. For the 5- or 10-yr average differences calculated below, we use Eq. (3) with $n = 5$ or 10, respectively.

3. Space–time patterns of Antarctic cooling

Time series of November 100-mb temperatures are shown in Fig. 3 for each of the eight Antarctic radiosonde locations. The low-frequency decadal trends show evidence of cooling since about 1985 at each station. The smoothed decadal variations for each radiosonde station are shown together in Fig. 4 for data during March, July, October, and November. Here temperature at each station is referenced with respect to a 1970–79 average of zero, and the appropriate decadal 2σ values [Eq. (3)] are also indicated (variability outside of 2σ indicates a significant departure from natural variability). This comparison highlights a significant decadal-scale cooling in spring after approximately 1985 with magnitude of 6–10 K, and shows that a similar variation is observed at most stations. Figure 4 furthermore shows that a smaller but significant cooling ($\sim$1 K) is observed in late summer (March), but that no significant change is observed during winter (July) (except for data from one station, SANAE). The midwinter cooling trends observed in data from SANAE are questionable in light of the lack of trends at any other station (particularly the nearby Halley Bay), and we do not include SANAE in the average seasonal statistics below.

Figure 5 shows a contour plot of the temperature changes between the time periods (1986–95 minus 1970–79), plotted versus altitude and month, with significant changes noted with shading. This is derived from an average over the stations shown in Fig. 3, with the exclusion of SANAE (as discussed above). Figure 5 shows cooling in the lower stratosphere ($\sim$200–50 mb; 12–21 km) throughout spring, with maximum (~ -6 K) near 100 mb in November. The maximum November cooling between these decades is closer to 8–10 K for most of the stations (see Fig. 4); McMurdo and Casey show smaller differences ($\sim$4 K) so that the average is somewhat above 6 K. Smaller magnitude (~ -1 K) but significant cooling extends throughout summer. These data also show evidence of warming in the uppermost data level (30 mb) during spring. Time

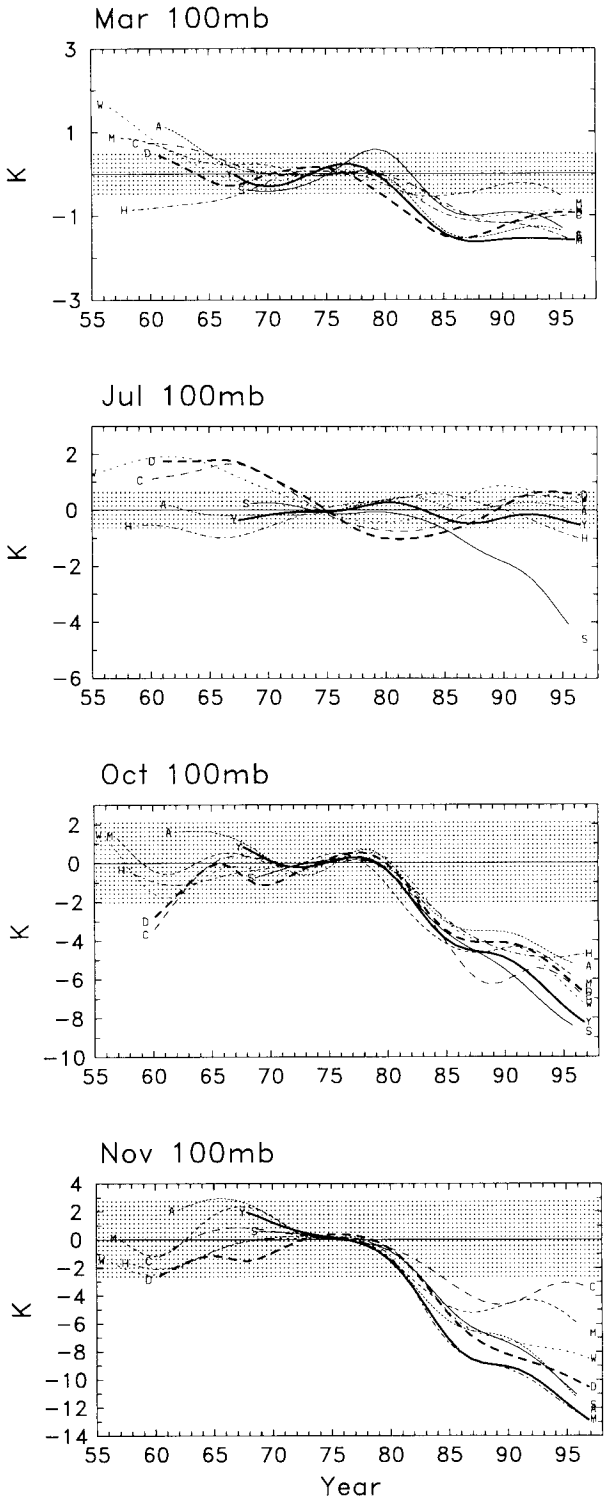

FIG. 4. Time series of smoothed 100-mb decadal temperature anomalies at each Antarctic radiosonde station shown in Fig. 3, for Mar, Jul, Oct, and Nov. The anomalies at each station are normalized to a zero mean over 1970–79. The shaded region in each panel indicates a ±2 sigma level of natural variability [using Eq. (3)].

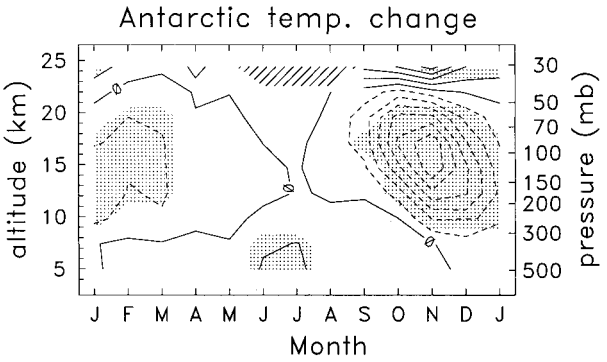

FIG. 5. Altitude–month profile of temperature differences between the decades (1986–95 minus 1970–79). Contour interval is 1 K, and shading denotes a 2-sigma statistically significant difference (with respect to natural variability). Data are unavailable during midwinter at the uppermost levels.

series of November 30-mb temperature are shown in Fig. 6 for McMurdo and Mawson, and Fig. 7 shows the 30-mb decadal variations for all stations in November and December. Although there is some variability between stations, a significant warming is clearly suggested. Figure 5 also shows warming of ~1 K in the upper troposphere (500–300 mb) during midwinter (June–July). This warming is seen at most of the individual stations, although its origin is unknown.

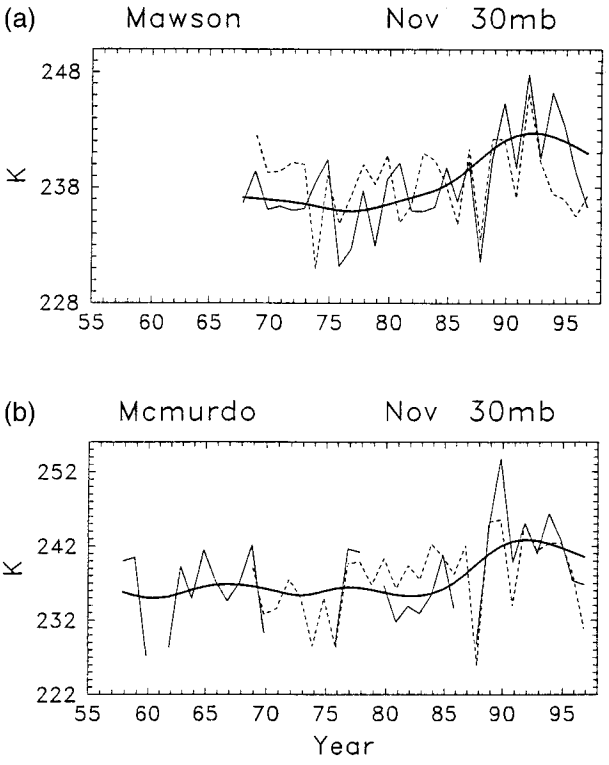

FIG. 6. Time series of Nov 30-mb temperature at (a) Mawson and (b) McMurdo. Line legend is the same as Fig. 3.

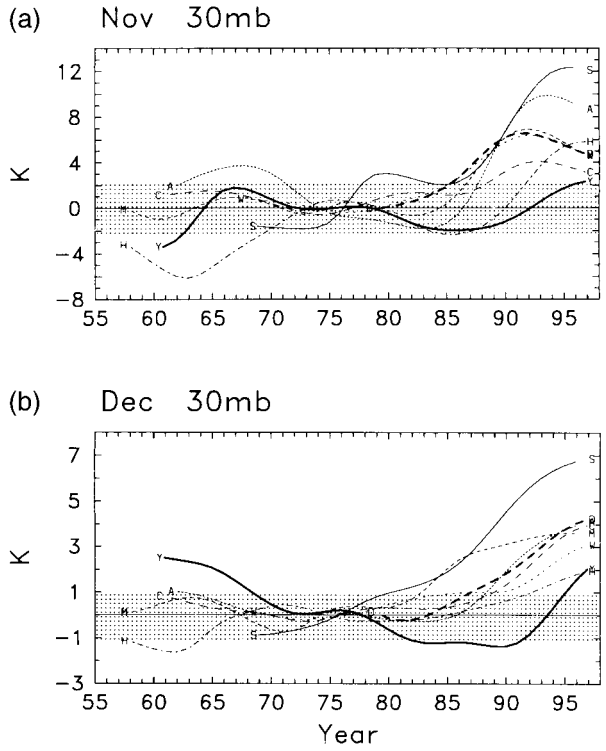

FIG. 7. Time series of smoothed 30-mb decadal temperature anomalies at each radiosonde station for Nov and Dec. The anomalies are normalized to a zero mean over 1970–79, and the shaded region indicates a ±2 sigma level of natural variability.

4. Arctic and Antarctic variability in MSU and reanalysis data

Figure 8 shows temperature trends as a function of latitude and month calculated from MSU data spanning January 1979–December 1997. These trends were calculated using a standard regression analysis, including terms modeling the 11-yr solar cycle and stratospheric quasibiennial oscillation (e.g., Randel and Cobb 1994). These data show maximum trends over SH polar regions in spring (September–December), in agreement with the radiosonde records analyzed above. The consistency of the MSU and Antarctic radiosonde records is illustrated in Fig. 9, where time series of November temperature anomalies from MSU (interpolated to the station locations) are compared with the vertical integral of radiosonde temperatures over 300–30 mb [using the MSU weighting function shown in Spencer and Christy (1993)]. There is reasonable agreement between interannual anomalies, although the agreement is not exact [and not as good as the midlatitude and tropical comparisons shown in Spencer and Christy (1993)]. This may be due to uncertainties in the exact weighting function structure, or neglect of radiosonde information above 30 mb (the upper level of regular reports). Comparison with the longer record of radiosonde data in Fig. 9 shows the clear decadal-scale cooling since the early 1980s.

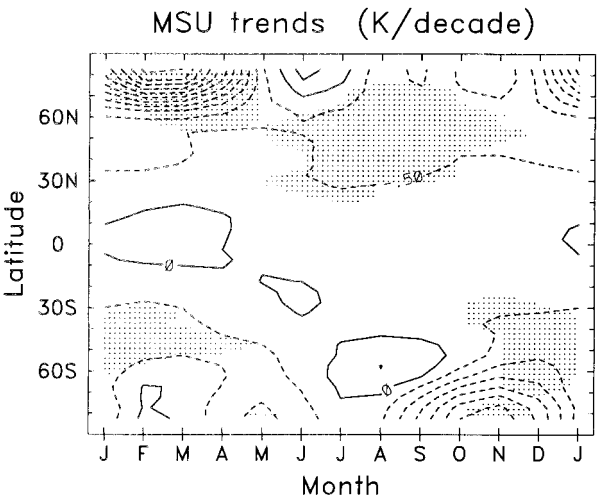

FIG. 8. Global temperature trends derived from MSU channel 4 data spanning 1979–97. Contour interval is 0.5 K per decade, and shading represents a 2-sigma significant trend.

The MSU data in Fig. 8 furthermore show strong cooling of the Arctic polar stratosphere during winter–spring (January–April), with somewhat larger trends (up to -5 K decade^{-1}) than in the SH. Small but statistically significant negative trends are observed over midlatitudes in both hemispheres during summer, and overall

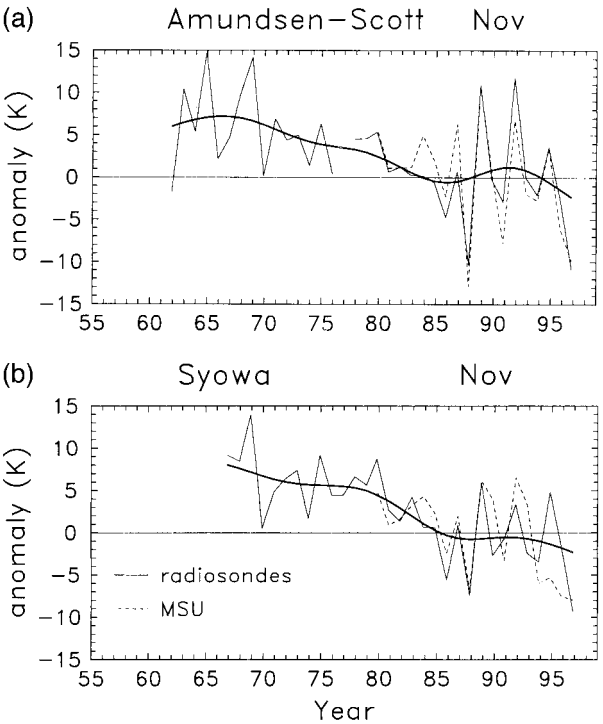

FIG. 9. Time series of MSU temperature anomalies (dashed lines) compared with the vertical integral of radiosonde data over 300–30 mb (using the MSU weighting function) at Amundsen–Scott and Syowa. The MSU data begin in 1979. The smooth curve shows the decadal variation of the radiosonde data.

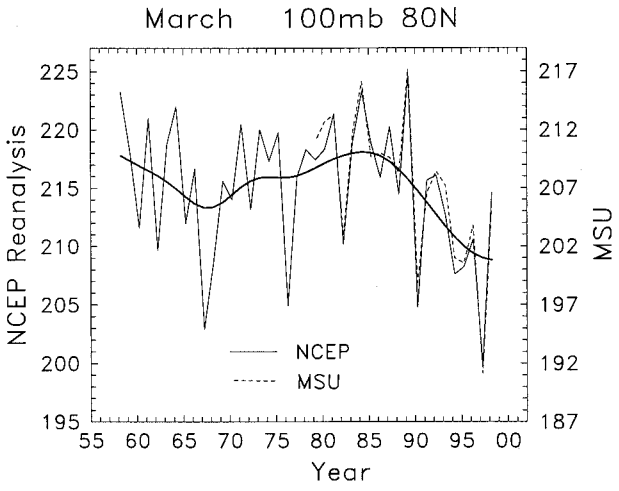

FIG. 10. Time series of March 100-mb zonal-mean temperatures at 80°N from NCEP reanalysis (1957–98) and MSU data (1979–98).

there is a high degree of global symmetry in lower-stratospheric temperature trends since 1979.

Time series of Arctic zonal-mean temperature anomalies in March at 80°N are shown in Fig. 10, from both NCEP reanalysis at 100 mb (1957–98) and MSU data (1979–98). Note there is a mean offset between the reanalyses at 100 mb and the MSU data (representative of the weighed average over ~150–50 mb), but this is unimportant as the focus here is on comparing interannual variations. These data are in good agreement in regards to interannual variability, both showing a substantial decline in temperature during the 1990s compared to prior climatology. March 1997 was the coldest on record in both datasets; March 1998 was somewhat warmer, but still ~3 K below the pre-1990 mean.

Figure 11 shows recent temperature changes versus altitude and month calculated from the reanalysis data. These temperature changes are calculated between the periods (1993–97 minus 1970–79), with results shown for 80°S (Fig. 11a) and 80°N (Fig. 11b). The time period 1993–97 is chosen because the strongest NH cooling has been observed only during the most recent years (see Fig. 10). Shaded regions in Fig. 11 denote statistical significance, using Eq. (3) (with $n = 5$) to evaluate natural variability for 5-yr means. The SH differences in Fig. 11a show reasonable agreement with the radiosonde differences shown in Fig. 5 (which were calculated for a slightly different time period), with a maximum cooling ~8 K near 100 mb in November. The reanalysis results in Fig. 11a (and the MSU trends in Fig. 8) show weak cooling during early winter (May–June) that is not observed in the radiosonde data. Figure 11b shows strong and statistically significant cooling (~−4 to −8 K) in the Arctic during January–April over much of the lower stratosphere, with a maximum in March. This Arctic cooling occurs about 2–3 months earlier in the season than the corresponding maxima in the SH. Note that in both polar regions the cooling does not extend into the troposphere (below 300 mb).

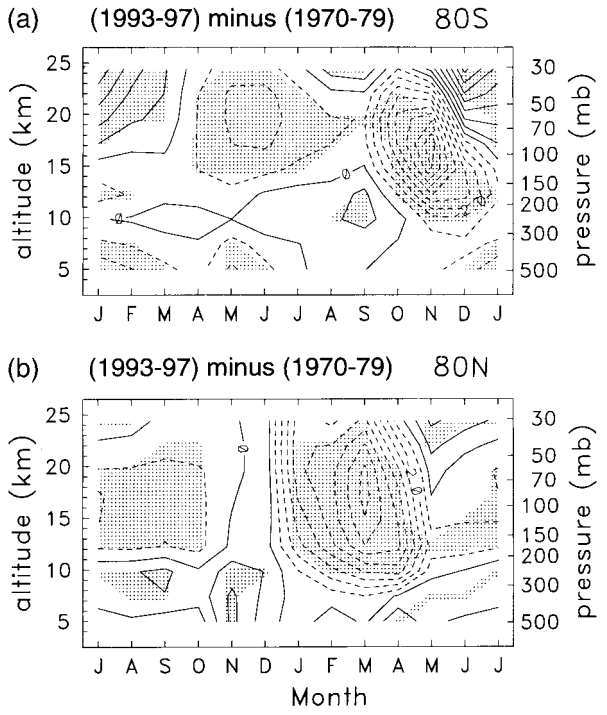

FIG. 11. Temperature differences for the time periods 1993–97 minus 1970–79, derived from the NCEP reanalysis data, for data at (a) 80°S and (b) 80°N Contour interval is 1 K, and shading denotes a statistically significant change (with respect to natural variability). Note the time axes are shifted by 6 months to facilitate direct seasonal comparisons.

Figure 12 shows the reanalysis temperature differences between the periods (1993–97 minus 1970–79) at 100 mb, plotted versus latitude and month. The pat-

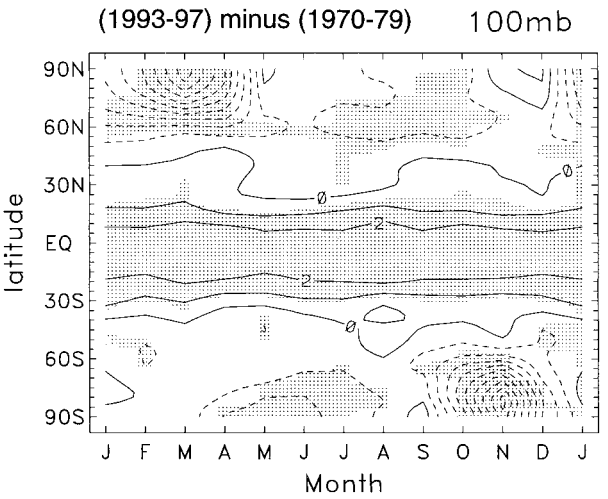

FIG. 12. Latitude–month plot of 100-mb temperature differences between the periods 1993–97 minus 1970–79, derived from NCEP reanalysis. Contour interval is 1 K.

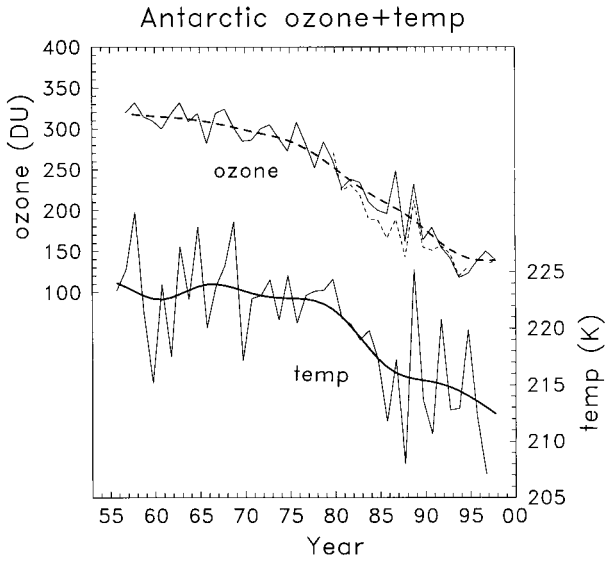

FIG. 13. (a) Time series of Oct average column ozone over Antarctica from ground-based Dobson (solid line) and TOMS satellite data (light dashed line). (b) Time series is the Oct 100-mb temperature over Antarctica, derived from an average of radiosonde data.

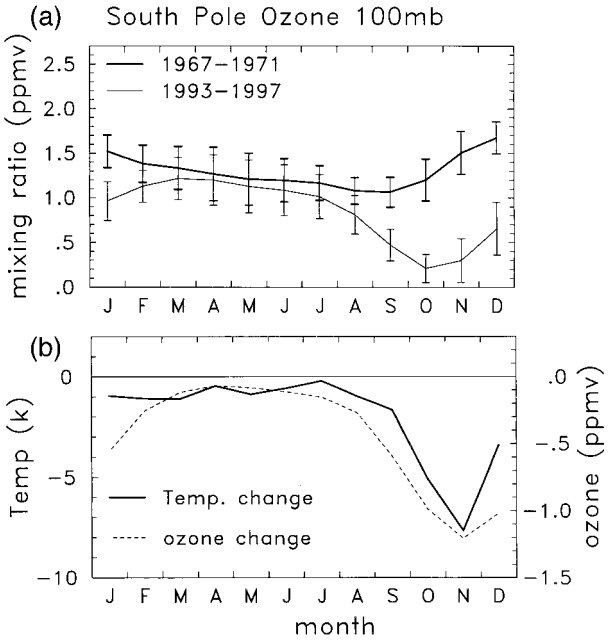

FIG. 14. (a) Seasonal behavior of ozone at 100 mb over the South Pole for the years 1967–71 and 1993–97. (b) Compares ozone changes between these periods (the difference of the upper two curves) with corresponding 100-mb temperature changes (derived from averaged radiosonde data).

terns here are similar to the MSU trends over 1979–97 (Fig. 8) in high latitudes, showing significant cooling in the springtime polar regions of each hemisphere. The latitudinal extent of the cooling covers approximately 60° to the pole in both hemispheres. The reanalysis results furthermore show a region of warming in the Tropics (~20°N–S) that is independent of season, and not observed in the MSU data (Fig. 8). Time series of temperatures in this region (not shown) reveal a clear jump in the data near 1978, when Tiros Operational Vertical Sounder satellite temperature retrievals were first available and incorporated into the analyses (Kalnay et al. 1996). This discontinuity appears in the Tropics near 100 mb, and extends into the SH midlatitudes (~40°–60°S) as low as 300 mb. The introduction of satellite data apparently makes a large impact over these primarily ocean-covered latitude bands due to the lack of sufficient radiosonde observations in the lower stratosphere. The higher density of radiosonde observations over the rest of the globe may help prevent such biases from being introduced (in particular, the springtime polar cooling in both hemispheres are not an artifact). This tropical discontinuity suggests caution in interpretation of decadal variability in the lower stratosphere based solely on the NCEP reanalysis.

5. Comparison of ozone and temperature changes

In this section we show some direct comparisons of the observed ozone and temperature changes, in particular comparing behavior in the NH versus SH. Figure 13 shows long-term observations of column ozone over Antarctica in October [ground-based Dobson data from Halley Bay (Jones and Shanklin 1995) and Total Ozone Mapping Spectrometer (TOMS) satellite data (Stolarski et al. 1997)] together with the 100-mb radiosonde temperature data in October, averaged over the eight stations in Fig. 3. Although the exact beginning of the ozone depletion is unclear, both ozone and temperature time series show rapid declines beginning in the early 1980s. The seasonal variation of the ozone and temperature changes at 100 mb are shown in Fig. 14. Figure 14a compares ozone mixing ratios at 100 mb over the South Pole for pre- and post-ozone-hole periods. These data were provided by S. Oltmans of the National Oceanic and Atmospheric Administration, and this figure is an update of Figs. 1–25 from WMO (1995). The lower panel in Fig. 14 compares the 100-mb ozone differences with 100-mb temperature differences [averaged radiosonde data, with differences calculated between (1993–97) minus (1970–79)]. The ozone data show largest differences during October–December, although significant losses are observed from August through February. The temperature data also show largest differences in October–December, with a maximum in November coinciding with the maximum in ozone loss; overall the ozone and temperature trends are approximately in phase. Figure 15 shows the vertical profile of ozone loss inside the ozone hole, derived from balloon measurements [from WMO (1995), adapted from Hofmann et al. 1994], together with the radiosonde cooling profile in November (1986–95 minus 1970–79 values, as in Fig. 5). This comparison shows that the temperature changes exhibit a vertical profile similar to that of ozone

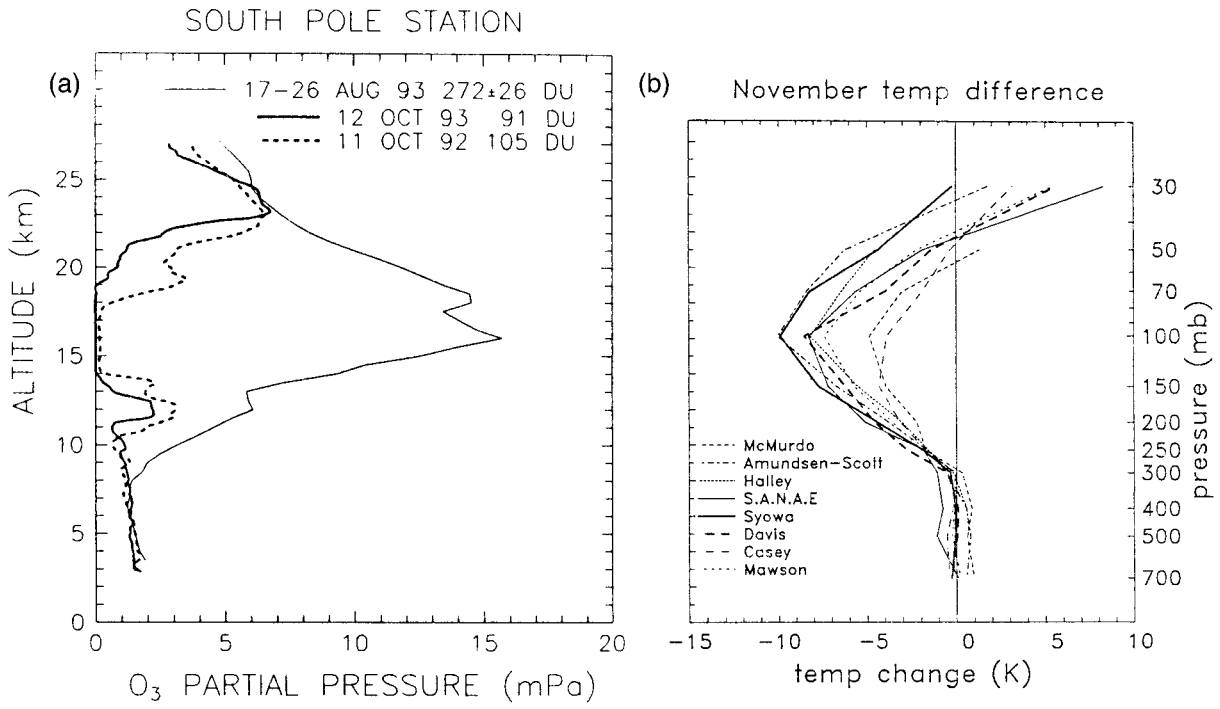

FIG. 15. (a) Vertical profile of ozone loss in the Antarctic ozone hole during 1992 and 1993 (from WMO 1995). (b) Vertical profile of temperature change during Nov from the Antarctic radiosondes (1986–95 minus 1970–79).

loss, with largest changes over the altitude range 12–21 km, and maxima near 16 km (~100 mb). Overall, Figs. 13–15 demonstrate a consistency between Antarctic ozone and temperature changes for decadal, seasonal, and vertical profile variations.

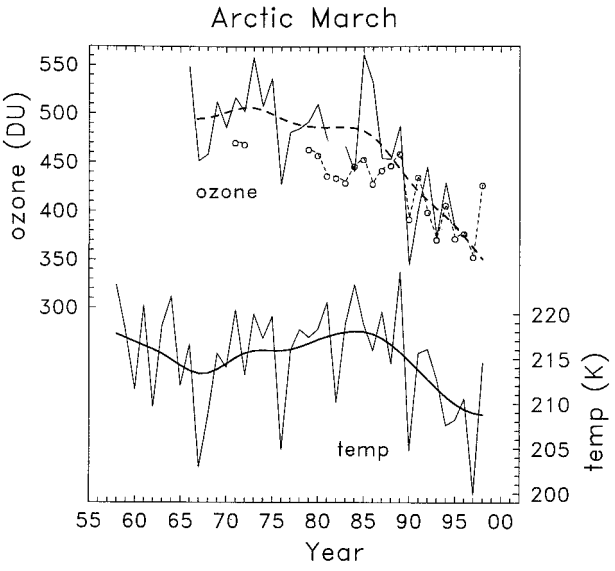

FIG. 16. Upper curves show time series of March average column ozone in the Arctic, including Dobson measurements at Resolute (75°N) (solid line) and satellite data poleward of 63°N [circles and dashed line—from Newman et al. (1997)]. Lower time series in the Mar 100-mb temperature at 80°N from NCEP reanalysis.

Figure 16 compares column ozone and 100-mb (reanalysis) temperature variations in March over the Arctic. The column ozone data include monthly mean Dobson measurements at Resolute (75°N), together with TOMS satellite data averaged poleward of 63°N (from Newman et al. 1997). These time series are in qualitative agreement, showing a clear decline in ozone during the 1990s. A very similar behavior is seen in the temperatures, which echo the year-to-year variability and also the decadal downward trend. Note the Arctic time series in Fig. 16 are similar to the Antarctic data shown in Fig. 13, but lagging in time by approximately a decade.

The seasonal variation of ozone and temperature changes in the Arctic lower stratosphere are shown in Fig. 17. The ozone data here are from ozonesonde measurements at Resolute (75°N), spanning 1966–97 (see Fioletov et al. 1997; these data were kindly provided by V. Fioletov). Figure 17a shows the 100-mb ozone amounts averaged over different time periods, showing a clear decline in recent years (1993–97) during January–April. Figure 17b directly compares these ozone differences with corresponding 100-mb temperature differences at 80°N (the same results as in Figs. 11–12). This comparison shows that the Arctic ozone and temperature changes are highly correlated and approximately in phase (very similar to the Antarctic results shown in Fig. 14). It is significant that ozone loss and cooling are both observed in the high-latitude Arctic in January, as this region is in polar night (see discussion below).

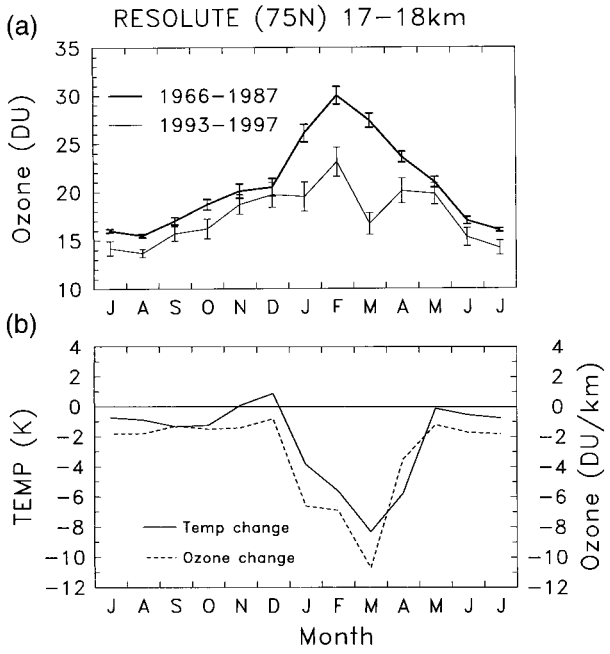

FIG. 17. (a) Seasonal behavior of ozone over 17–18 km (near 100 mb) at Resolute (75°N) for data over 1966–87 and 1993–97 (courtesy of V. Fioletov). (b) The ozone differences between 1993–97 minus 1966–87, together with the 100-mb temperature change at 80°N between 1993–97 minus 1970–79, derived from NCEP reanalysis.

6. Summary and discussion

Prior studies of temperature trends in the Antarctic stratosphere have shown springtime cooling (Trenberth and Olson 1989; Hurrell and van Loon 1994; Jones and Shanklin 1995). The analyses here have used long-term, updated radiosonde records from many stations to quantify the temporal and altitude structure of these Antarctic temperature changes. These radiosonde data show a near steplike temperature change between pre-1980 and post-1985 data. Cooling is observed throughout the lower stratosphere in spring, with a maximum (of order 6–10 K) near 100 mb in November. Smaller magnitude cooling (~1 K) persists throughout summer, and this cooling is statistically significant with respect to the small natural variability in the summer stratosphere. No significant stratospheric temperature changes are observed during SH winter. A warming is observed at the uppermost data level (30 mb) in spring.

Comparisons between the Antarctic radiosonde data and MSU satellite temperatures show good overall agreement. Although the MSU data extend back to only 1979, trends calculated since that time are consistent with the longer radiosonde data record (because the decadal changes occurred after 1980). The NCEP reanalysis also shows reasonable agreement with the radiosonde and MSU data for decadal trend variations. The MSU and NCEP data show that the springtime cooling is largely confined to the polar cap region (~60°S–pole).

The observed Antarctic temperature changes exhibit similar decadal, seasonal, and altitude behavior to that observed for ozone depletion (Figs. 13–15). The link between ozone loss and springtime temperature changes is made stronger by comparison with results from model simulations. A number of studies have imposed an ozone hole in a GCM to study the radiative and dynamical response (Kiehl et al. 1988; Cariolle et al. 1990; Mahlman et al. 1994; Ramaswamy et al. 1996; Shindell et al. 1997; Graf et al. 1998). These studies have produced similar overall results, namely a cooling of the lower stratosphere in spring with magnitude ~5–10 K, coupled with a warming of the upper stratosphere by ~5 K. Shindell et al. (1997) show substantial interannual variability in temperature (and ozone depletion), due to variations in planetary wave forcing in the model troposphere. A similar variability is observed in the real atmosphere (see Fig. 1), and this mandates relatively long time series before the decadal-scale changes can be isolated.

Stratospheric temperatures are also expected to decrease as a result of greenhouse gas increases (e.g., Rind et al. 1990; Tett et al. 1996; Graf et al. 1998). However, the predicted magnitude of such changes in the lower stratosphere for present conditions is of order ~ -0.5 K (Tett et al. 1996), which is an order of magnitude smaller than the springtime changes documented here. Shindell et al. (1998) have recently found stronger Arctic temperature changes in a GCM simulation of greenhouse gas increases, due to a feedback from changes in planetary wave propagation. However, such a strong seasonal signature is not reproduced in other model simulations at present.

The MSU and reanalysis data furthermore show strong decadal temperature trends in the Arctic lower stratosphere in winter–spring. This recent cooling of the NH lower stratosphere during winter (and intensification of the polar vortex) has been discussed by Zurek et al. (1996), Naujokat and Pawson (1996), Pawson and Naujokat (1997), and Coy et al. (1997). The cooling in the Arctic is strongest in the 1990s, and shows similar decadal and seasonal dependence to the observed NH spring ozone depletions (Figs. 16–17). There is an overall similarity in space–time structure of the ozone loss and cooling patterns that suggests the Arctic changes are similar to those observed in the Antarctic one decade earlier. Note especially that the coupled seasonal variations in Arctic ozone and temperature (Fig. 17) are similar to the variations seen in the Antarctic (Fig. 14). Although detailed model simulations have not been performed to date, the observed patterns suggest that the radiative response to ozone loss is likely important for the Arctic as well. Ramaswamy et al. (1996) and Graf et al. (1998) have calculated the response to global ozone loss using GCM simulations with imposed TOMS column ozone trends, together with assumptions regarding the vertical profile and trends in polar night. Their results show strong Arctic cooling in late spring (April–May), but not in winter (as observed here). How-

ever, the imposed ozone trends in these runs did not include strong ozone losses in winter [like those observed in January–February at Resolute (Fig. 17)], because of lack of TOMS data in polar night. Hence it is not straightforward to compare those simulations with the Arctic observations here.

In spite of the overall similarity between hemispheres, there is one important distinction between the NH and SH polar cooling patterns. While the SH cooling occurs primarily in spring (after the sun returns), there is cooling observed in the NH throughout winter–spring (January–April; see Figs. 11 and 17). The NH winter ozone loss and cooling occurs prior to the time when the sun returns to high latitudes (early February at 75°N), and there are several possible interpretations. First, ozone depletion in polar night can still cause a thermal response in the lower stratosphere, because ozone absorbs a significant amount of infrared radiation from the troposphere (Ramanathan and Dickinson 1979). Also, because the Arctic polar vortex is often highly asymmetric, air parcels experience large latitudinal excursions and air with mean latitude of 75°N may see substantial sunlight during the month (and hence be subject to ozone ultraviolet heating). This is a mechanism that could also produce photochemical ozone depletion. There is also evidence that the Arctic stratospheric cooling is linked to tropospheric dynamical variability. Coy et al. (1997) note a decrease in planetary wave forcing from the troposphere, correlated with the recent cooling. The recent studies of Kodera and Yamazaki (1994), Graf et al. (1995), Kodera and Koide (1997), and Thompson and Wallace (1998, 1999, manuscript submitted to *J. Climate*) find coherence between polar stratospheric temperature changes and large-scale tropospheric circulation anomalies, suggesting a low-frequency oscillation of the NH winter climate extending into the lower stratosphere. Such circulation changes would also be expected to influence ozone, in a manner coherent with temperature changes (e.g., Randel and Cobb 1994). It is not straightforward to separate such dynamical temperature changes from those associated with a radiative response to ozone losses in the NH. We simply point out that there is a strong similarity in polar temperature and ozone trends between hemispheres, and this suggests that some component of the NH spring cooling is attributable to ozone loss.

Because chemical ozone depletion over polar regions is related to the presence of cold temperatures (below approximately 195 K; see WMO 1999) and sunlight, any winter or springtime cooling due to ozone loss radiative effects has the potential for positive feedback (i.e., ozone loss → colder temperatures → more ozone loss). This effect is clearly demonstrated in the modeling results of Austin et al. (1992), where this mechanism led to chronic Arctic ozone hole formation in a doubled CO_2 climate simulation. The effectiveness of such a feedback is related to how the radiative temperature change affects the seasonal cycle of temperature, in particular in relation to the ~195 K threshold; such a threshold is well correlated with chemical ozone depletion (see Chipperfield and Pyle 1998). Figure 18 shows the seasonal cycle of average minimum temperatures over the SH and NH for the years 1970–79 and 1993–97, calculated from NCEP reanalysis. Here the daily minimum temperature has been calculated for each year of the respective time periods, and then averaged over these years. There is a large degree of year-to-year variability in minimum temperatures (see Pawson and Naujokat 1997; Chipperfield and Pyle 1998); these long-term averages are intended to illustrate how the decadal temperature changes discussed above influence minimum temperatures (and possibly ozone loss). The springtime temperature change in the SH in Fig. 18 results in a relatively small delay (~1 week) in crossing the 195-K threshold in October. In contrast, the recent temperature changes in the NH strongly increase the average amount of time spent below 195 K, because the seasonal cycle was previously close to this threshold. The cold zonal-mean conditions in March 1997 (Fig. 10) were associated with minimum temperatures below 195 K throughout much of the month; this was a strong departure from climatological conditions (Coy et al. 1997; Santee et al. 1997). Consistent with these cold

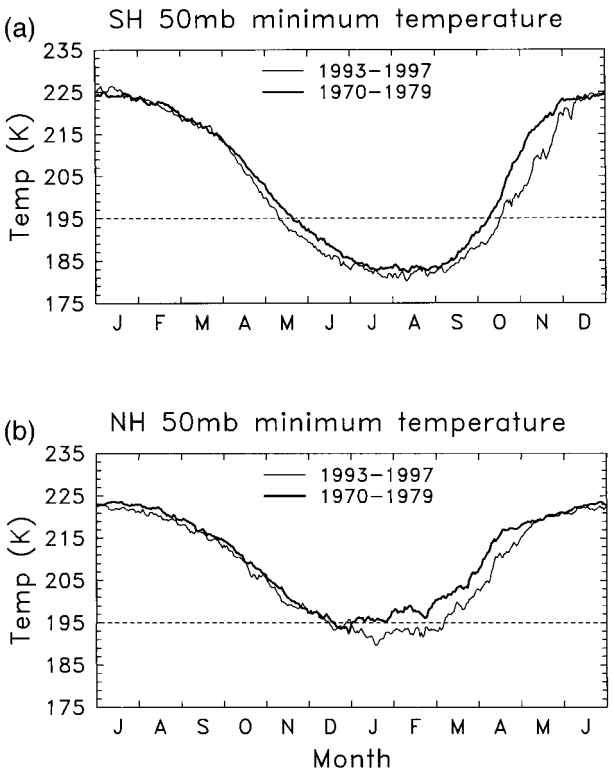

FIG. 18. Seasonal march of hemispheric minimum temperatures for (a) the SH and (b) NH, averaged over the years 1970–79 and 1993–97. These results are based on NCEP reanalysis. Daily minimum temperatures are calculated for each year and then averaged over the 5- or 10-yr samples.

temperatures, measurements of reactive chlorine at 80°N (Donovan et al. 1997) showed elevated levels throughout March, confirming a chemical loss mechanism contributing to the observed low ozone [as modeled in the simulations of Chipperfield and Pyle (1998) and Lefevre et al. (1998).]

A second type of feedback effect is related to the influence of springtime cooling on polar vortex structure and ozone transport. A colder and more intense (and more persistent) polar vortex is associated with less dynamical transport of ozone from the tropical photochemical source region into high latitudes. Manney et al. (1997) have concluded that the anomalously strong Arctic vortex in spring 1997 was a dominant factor for the observed low polar ozone, while Lefevre et al. (1998) calculate that up to half of the 1997 ozone reduction was due to weakened transport. Furthermore, Zurek et al. (1996), Coy et al. (1997), and Waugh and Randel (1999) have documented an intensification and enhanced persistence of the lower-stratospheric Arctic vortex in spring during the 1990s, consistent with the cooling documented above. To the extent that ozone radiative effects contribute to the observed NH cooling in winter and spring, they also contribute to a stronger vortex and relatively less dynamical transport of ozone. Again, the recent changes will have relatively stronger impact in the NH, because ozone transport is stronger and relatively more important than in the SH.

In summary, both chemical and dynamical feedback effects associated with low temperatures may contribute to springtime ozone reduction. However, it is difficult to separate chemical versus transport effects on ozone, and hard to identify feedback effects in observed data (particularly given the large degree of natural interannual variability in the NH). What is clear from observations is that on a decadal timescale 1) NH ozone levels have decreased during spring, and 2) temperatures have cooled and the polar vortex becomes stronger. More specific attribution of cause and effect will require extensive modeling studies.

Acknowledgments. This work was begun while the first author was on sabbatical leave at the Cooperative Research Center for Southern Hemisphere Meteorology in Melbourne, Australia. The ozone data in Fig. 17 were kindly provided by Vitali Fioletov. Resolute ozone data were obtained from the World Ozone and Ultraviolet Radiation Data Center (WOUDC). Thanks to Sam Oltmans for providing updated South Pole ozone data. We thank Kevin Trenberth, Jim Hurrell, Mike Coffey, and Mark Schoeberl for discussions and constructive reviews of the manuscript. Partial support was provided under NASA Grants W-18181 and W-16215. The National Center for Atmospheric Research is sponsored by the National Science Foundation.

REFERENCES

Angell, J. K., 1986: The close relation between Antarctic total ozone depletion and cooling of the Antarctic low stratosphere. *Geophys. Res. Lett.,* **13,** 1240–1243.

Austin, J., N. Butchart, and K. P. Shine, 1992: Possibility of an Arctic ozone hole in a doubled-CO_2 climate. *Nature,* **360,** 221–225.

Blackman, R. B., and J. W. Tukey, 1958: *The Measurement of Power Spectra.* Dover, 190 pp.

Cariolle, D. A., A. Lasserre-Bigorry, J. F. Royer, and J. F. Geleyn, 1990: A general circulation model simulation of the springtime Antarctic ozone decrease and its impact on midlatitudes. *J. Geophys. Res.,* **95,** 1883–1898.

Chipperfield, M. P., and J. A. Pyle, 1998: Model sensitivity studies of Arctic ozone depletion. *J. Geophys. Res.,* **103,** 28 389–28 403.

Chubachi, S., 1986: On the cooling of stratospheric temperatures at Syowa, Antarctica. *Geophys. Res. Lett.,* **13,** 1221–1223.

Coy, L., E. R. Nash, and P. A. Newman, 1997: Meteorology of the polar vortex: Spring 1997. *Geophys. Res. Lett.,* **24,** 2693–2696.

Donovan, D. P., and Coauthors, 1997: Ozone, column ClO, and PSC measurements made at the NDSC Eureka observatory (80°N, 86°W) during the spring of 1997. *Geophys. Res. Lett.,* **24,** 2709–2712.

Farman, J. C., B. G. Gardiner, and J. D. Shanklin, 1985: Large losses of total ozone in Antarctica reveal seasonal ClO_x/NO_x interaction. *Nature,* **315,** 207–210.

Fioletov, V. E., J. B. Kerr, D. I. Wardle, J. Davies, E. W. Hare, C. T. McElroy, and D. W. Tarasick, 1997: Long-term ozone decline over the Canadian Arctic to early 1997 from ground-based and balloon observations. *Geophys. Res. Lett.,* **24,** 2705–2708.

Graf, H.-F., J. Perlwitz, I. Kirchner, and I. Schult, 1995: Recent northern winter climate trends, ozone changes and increased greenhouse gas forcing. *Beitr. Phys. Atmos.,* **68,** 233–248.

——, I. Kirchner, and J. Perlwitz, 1998: Changing lower stratospheric circulation: The role of ozone and greenhouse gases. *J. Geophys. Res.,* **103,** 11 251–11 261.

Hofmann, D. J., S. J. Oltmans, J. A. Lathrop, J. M. Harris, and H. Voemel, 1994: Record low ozone at the South Pole in the spring of 1993. *Geophys. Res. Lett.,* **21,** 421–424.

——, ——, J. M. Harris, B. J. Johnson, and J. A. Lathrop, 1997: Ten years of ozonesonde measurements at the South Pole: Implications for recovery of springtime Antarctic ozone loss. *J. Geophys. Res.,* **102,** 8931–8943.

Hurrell, J. W., and H. van Loon, 1994: A modulation of the atmospheric annual cycle in the Southern Hemisphere. *Tellus,* **46A,** 325–338.

Jones, A. E., and J. D. Shanklin, 1995: Continued decline of total ozone over Halley, Antarctica since 1985. *Nature,* **376,** 409–411.

Kalnay, E., and Coauthors, 1996: The NCEP/NCAR 40-Year Reanalysis Project. *Bull. Amer. Meteor., Soc.,* **77,** 437–471.

Kiehl, J. T., B. A. Boville, and B. P. Briegleb, 1988: Response of a general circulation model to a prescribed Antarctic ozone hole. *Nature,* **332,** 501–504.

Kodera, K., and K. Yamazaki, 1994: A possible influence of polar stratospheric coolings on the troposphere in the Northern Hemisphere winter. *Geophys. Res. Lett.,* **21,** 809–812.

——, and H. Koide, 1997: Spatial and seasonal characteristics of recent decadal trends in the Northern Hemisphere troposphere and stratosphere. *J. Geophys. Res.,* **102,** 19 433–19 447.

Koshelkov, Y. P., E. N. Kovshova, and A. I. Voskresensky, 1992: Seasonal aspects of long-term temperature trends in the lower Antarctic stratosphere. *Extended Abstracts, Int. Symp. on Middle Atmospheric Science,* Kyoto, Japan, Scientific Committee on Solar-Terrestrial Physics (SCOSTEP). 125–126.

Lefevre, F., F. Figarol, K. S. Carslaw, and T. Peter, 1998: The 1997 Arctic ozone depletion quantified from three-dimensional model simulations. *Geophys. Res. Lett.,* **25,** 2425–2428.

Mahlman, J. D., J. P. Pinto, and L. J. Umscheid, 1994: Transport, radiative and dynamical effects of the Antarctic ozone hole: A

GFDL ''SKYHI'' model experiment. *J. Atmos. Sci.,* **51,** 489–508.

Manney, G. L., R. Swinbank, S. T. Massie, M. E. Gelman, A. J. Miller, R. Nagatani, A. O'Neill, and R. W. Zurek, 1996: Comparison of U.K. Meteorological Office and U.S. National Meteorological Center stratospheric analyses during northern and southern winter. *J. Geophys. Res.,* **101,** 10 311–10 334.

——, L. Froidevaux, M. L. Santee, R. W. Zurek, and J. W. Waters, 1997: MLS observations of Arctic ozone loss in 1996–97. *Geophys. Res. Lett.,* **24,** 2697–2700.

Mo, K. C., X. L. Wang, R. Kistler, M. Kanamitsu, and E. Kalnay, 1995: Impact of satellite data on the CDAS-reanalysis system. *Mon. Wea. Rev.,* **123,** 124–139.

Naujokat, B., and S. Pawson, 1996: The cold stratospheric winters 1994/95 and 1995/96. *Geophys. Res. Lett.,* **23,** 3703–3706.

Newman, P. A., and M. R. Schoeberl, 1986: October Antarctic temperature and total ozone trends from 1979–1985. *Geophys. Res. Lett.,* **13,** 1206–1209.

——, and W. J. Randel, 1988: Coherent ozone-dynamical changes during the Southern Hemisphere spring, 1979–1986. *J. Geophys. Res.,* **93,** 12 585–12 606.

——, J. F. Gleason, R. D. McPeters, and R. S. Stolarski, 1997: Anomalously low ozone over the Arctic. *Geophys. Res. Lett.,* **24,** 2689–2692.

Pawson, S., and B. Naujokat, 1997: Trends in daily wintertime temperatures in the northern stratosphere. *Geophys. Res. Lett.,* **24,** 575–578.

Ramanathan, V., and R. E. Dickinson, 1979: The role of stratospheric ozone in the zonal and seasonal radiative energy balance of the Earth-troposphere system. *J. Atmos. Sci.,* **36,** 1084–1104.

Ramaswamy, V., M. D. Schwarzkopf, and W. J. Randel, 1996: Fingerprint of ozone depletion in the spatial and temporal pattern of recent lower stratospheric cooling. *Nature,* **382,** 616–618.

Randel, W. J., 1988: The anomalous circulation in the Southern Hemisphere stratosphere during spring 1987. *Geophys. Res. Lett.,* **15,** 911–914.

——, and J. B. Cobb, 1994: Coherent variations of monthly mean total ozone and lower stratospheric temperature. *J. Geophys. Res.,* **99,** 5433–5447.

Rind, D., R. Suozzo, N. K. Balachandvan, and M. J. Prather, 1990: Climate change and the middle atmosphere. Part I: The doubled CO_2 climate. *J. Atmos. Sci.,* **47,** 475–494.

Santee, M. L., G. L. Manney, L. Froidevaux, R. W. Zurek, and J. W. Waters, 1997: MLS observations of ClO and HNO_3 in the 1996–97 Arctic polar vortex. *Geophys. Res. Lett.,* **24,** 2713–2716.

Sekiguchi, Y., 1986: Antarctic ozone change correlated to the stratospheric temperature field. *Geophys. Res. Lett.,* **13,** 1202–1205.

Shindell, D. T., S. Wong, and D. Rind, 1997: Interannual variability of the Antarctic ozone hole in a GCM. Part I: The influence of tropospheric wave variability. *J. Atmos. Sci.,* **54,** 2308–2319.

——, D. Rind, and P. Lonergan, 1998: Increased polar stratospheric ozone losses and delayed eventual recovery owing to increasing greenhouse-gas concentrations. *Nature,* **392,** 589–592.

Shine, K. P., 1986: On the modeled thermal response of the Antarctic stratosphere to a depletion of ozone. *Geophys. Res. Lett.,* **13,** 1331–1334.

Solomon, S., 1988: The mystery of the Antarctic ozone ''hole.'' *Rev. Geophys.,* **26,** 131–148.

Spencer, R. W., and J. R. Christy, 1993: Precision lower stratospheric temperature monitoring with the MSU: Technique, validation and results 1979–1991. *J. Climate,* **6,** 1194–1204.

Stolarski, R. S., A. J. Krueger, M. R. Schoeberl, R. D. McPeters, P. A. Newman, and J. C. Alpert, 1986: *Nimbus 7* satellite measurements of the springtime Antarctic ozone decrease. *Nature,* **322,** 308–311.

——, G. J. Labow, and R. D. McPeters, 1997: Springtime Antarctic total ozone measurements in the early 1970's from the BUV instrument on *Nimbus 4. Geophys. Res. Lett.,* **24,** 591–594.

Tett, S. F. B., J. F. B. Mitchell, D. E. Parker, and M. R. Allen, 1996: Human influence on the atmospheric vertical temperature structure: Detection and observations. *Science,* **274,** 1170–1173.

Thompson, D. W. J., and J. M. Wallace, 1998: The Arctic Oscillation signature in wintertime geopotential height and temperature fields. *Geophys. Res. Lett.,* **25,** 1297–1300.

Trenberth, K. E., and J. G. Olson, 1989: Temperature trends at the South Pole and McMurdo Sound. *J. Climate,* **2,** 1196–1206.

Waugh, D. W., and W. J. Randel, 1999: Climatology of Arctic and Antarctic polar vortices using elliptical diagnostics. *J. Atmos. Sci.,* in press.

Wirth, V., 1993: Quasi-stationary planetary waves in total ozone and their correlation with lower stratospheric temperature. *J. Geophys. Res.,* **98,** 8873–8882.

WMO, 1995: Scientific assessment of ozone depletion: 1994, Global Ozone Research and Monitoring Project. Rep. 37, World Meteorological Organization.

——, 1999: Scientific assessment of ozone depletion: 1998, Global Ozone Research and Monitoring Project. Rep. 44, World Meteorological Organization.

Zurek, R. W., G. L. Manney, A. J. Miller, M. E. Gelman, and R. M. Nagatani, 1996: Interannual variability of the north polar vortex in the lower stratosphere during the UARS mission. *Geophys. Res. Lett.,* **23,** 289–292.